Relaxational dynamics of supercooled water in porous glass

J.-M. Zanotti,[1] M.-C. Bellissent-Funel,[1] and S.-H. Chen[2]

[1]*Laboratoire Léon Brillouin (CEA-CNRS), CEA Saclay, 91191 Gif-sur-Yvette, France*
[2]*Department of Nuclear Engineering, 24-209, Massachusetts Institute of Technology, Cambridge, Massachusetts 02139*

(Received 14 July 1998)

We have made a high-resolution quasielastic incoherent neutron scattering (QENS) study of the translational dynamics of supercooled water contained in micropores of Vycor glass at different hydration levels. QENS spectra from the confined H_2O are analyzed in terms of the α-relaxation dynamics predicted by mode-coupling theory of supercooled liquids and by a recent computer molecular-dynamics simulation of extended simple point charge model water. We verify that the stretched exponential relaxation description of the long-time test-particle dynamics is consistent with the measured QENS spectral line shape. We are thus able to determine the wave-number dependence of magnitudes of the structural relaxation rate $1/\tau$ and the stretch exponent β as functions of temperature and coverage. A power-law dependence of the average relaxation time on the magnitude of the scattering vector Q is observed. In the Q range studied, the exponent starts out with nearly -2.0, at room temperature, indicating a continuous diffusion, and gradually becomes less negative as the temperature is decreased to below the freezing temperature.
[S1063-651X(99)13302-6]

PACS number(s): 61.25.−f, 68.45.−v

I. INTRODUCTION

Single-particle dynamics of bulk water has been extensively studied over a wide range of temperatures at ambient pressure. In particular, many investigations using techniques such as incoherent quasielastic (QENS) and inelastic neutron scattering (INS) [1–4], coherent inelastic neutron [5] and x-ray scattering (IXS) [6], and computer molecular-dynamics (MD) simulations been performed in a supercooled regime [7–10], where the effects due to hydrogen bondings are dominant. However, in many relevant situations, water is not in its bulk form but attached to some substrates or filling small cavities. Common examples are water in porous media, water in the interior of biological cells or on surfaces of proteins and lipid bilayers. We shall call water in the latter environment an ''interfacial water'' as opposed to a bulk water.

Traditionally, the diffusional dynamics of interfacial water, in particular that of water in the hydration layer of proteins, has been studied by nuclear magnetic relaxation dispersion technique. Halle and co-workers [11] have shown that oxygen-17 and deuteron spin relaxation rate in water is dominated by quadrupolar coupling to the electric field gradient of the intramolecular origin. Thus it is a particularly suitable method for investigating single-particle dynamics of interfacial water. Their general findings are summarized as follows: (a) perturbation (orientation and rotation) of the single-particle dynamics confined to water molecules in direct contact with the surface; (b) reorientation correlation time slows down by a factor between 2 and 8 times compared to the bulk water; (c) reduced lateral mobility (10–100 times); (d) long residence time in the first hydration shell (10–50 ps), in agreement with an estimate from multidimensional nuclear Overhauser enhancement spectroscopy (NOESY) [12].

Results of MD simulations [13,14] generally agreed that the dynamics of water molecules on protein and silica surfaces suffers only a mild slowing down compared to that of bulk water. More specifically, Rossky and Lee reported that the slowing down is about a factor 2 in the protein case and about a factor 5 in the silica case. Residence times of water in the first hydration layer are typically about 100 ps [14].

From the above comparison it seems clear that there is considerable uncertainty in the knowledge of diffusional dynamics obtained from NMR experiments and MD simulations. This is especially true for the translational diffusion constant. In this paper we would like to explore to what extent one can learn about the Q-dependent translational diffusion of water in bulk supercooled states and near a hydrophilic surface. On previous occasions, we argued that dynamics of interfacial water is similar to that of a bulk supercooled water at a lower temperature [15,16]. In essence the intermediate scattering function of the translational motion of water can be put into a scaling form in which the scaling parameter is the structural relaxation time that depends on temperature and on the dimensionality of the environment.

In a previous paper [17], we have reported the results of a model analysis of incoherent quasielastic and inelastic neutron scattering of water in Vycor at several temperatures starting from room temperature down to $-35\,°C$ and for the cases of 100%, 52%, and 25% hydrations. The experiment was done with a time-of-flight spectrometer (Mibemol at Saclay, France) having a medium energy resolution of 28 μeV [full width at half maximum (FWHM)]. The analysis was based on modeling the single-particle dynamics of water as a continuous diffusion process in a confined geometry of a sphere of radius a. The essence of the theory is to regard the low-frequency incoherent scattering spectrum as composed of a weighted sum of an elastic line and a quasielastic line which is Lorentzian in shape. The weighting factor is the elastic incoherent structure factor (EISF) which is the square

of the Fourier transform of the equilibrium spatial distribution function of molecules inside the confining volume. The Q-dependent EISF's extracted from the analysis were consistent with a confining radii of 3.5–4.5 Å, depending on temperature and hydration level. These confinement radii are less than one-tenth of the known average pore size in Vycor, which is 50 Å. It is obvious that in the time scale of typical QENS measurements (tens of ps range), the molecules do not have sufficient time to explore all the available space inside the porous glass. Even allowing for this fact, the existence of a purely elastic line is not a plausible concept in liquids. One is more at ease with an idea that the translational degree of freedom is never completely suppressed in the liquid state.

In this paper we shall introduce an idea of local structural relaxation into the description of diffusional dynamics in supercooled and interfacial water. In supercooled or interfacial water, due to the reduced thermal energy of the molecule, and for water, due to the formation of a stabler, tetrahedrally coordinated, hydrogen-bonded neighboring shells around each molecule, a molecule can translate a substantial distance only by rearranging positions of a large number of molecules around it. Thus the diffusion is strongly coupled to the local structural rearrangements or the structural relaxation. The usual, Markovian, Brownian-like diffusion process is no longer valid in the case of supercooled water. This is clearly shown in the recent long-time MD simulation of extended simple point charge (SPC/E) supercooled water [7–10].

II. TRANSLATIONAL MOTION OF WATER IN A CONFINED SPACE

Water is a triatomic, symmetric molecule, consisting of two light hydrogen atoms and a heavy oxygen atom. Its center of mass is very nearly at the position of the oxygen atom. While the incoherent neutron cross section of an oxygen atom is zero, that of individual hydrogen is about 80 barn and dominates the observed scattering cross section. Thus, as far as a QENS experiment of light water is concerned, we need only consider motions of an individual hydrogen atom. Motions of a H atom are composed of three components: vibrational motion of the atom around its equilibrium position, rotational motion of the atom around the water center of mass, and the translational motion of the center of mass. It has been generally assumed in the literature that, for the purpose of calculating the QENS cross section, the intermediate scattering function (ISF) of the H atom is a product of three factors each representing the time correlation function of the component motion. This simplification is called the ''decoupling approximation'' [2]. First of all, the time scale of observation of typical QENS spectra ($1.0 < t < 100$ ps) is much longer than the vibrational period of the hydrogen atom. In this long-time limit, the vibrational ISF is effectively reduced to a Debye-Waller factor. For a high-resolution QENS experiment, the magnitude of the scattering wave vector Q is always less than 1 Å^{-1}. Since the equilibrium O-H bond is about 1 Å, the vibrational amplitude of the hydrogen atom around its equilibrium position cannot be larger than 0.1 Å. Under this circumstance, the Debye-Waller factor is nearly unity and thus the vibrational contribution drops out of consideration. This means that for the

purpose of analyzing a QENS spectrum, a water molecule can be treated as a rigid molecule. The second issue concerning us here is the validity of the decoupling approximation. In a recent extensive computer molecular-dynamics (MD) simulation of SPC/E model water (rigid molecule) at supercooled temperatures, Chen et al. [9] showed that the decoupling approximation is good to a few percent for Q less than 1 Å^{-1}, even though the rotational and translational motions of a water molecule are strongly coupled at all time. The most interesting point of observation from the MD simulation is that for time longer than about 1 ps, the ISF of the H atom is closely approximated by that of the translational ISF alone. In the frequency domain, the dynamic structure factor calculated from the ISF of the H atom is equal to that calculated from the translational ISF alone plus a very small constant background coming from the convolution with the Fourier transform of the rotational ISF. This means that for all practical purpose, for analysis of a high-resolution QENS spectrum, we need only to have a theoretical expression for the translational ISF. This results in a great deal of simplification for the analysis of a QENS spectrum.

A detailed discussion of the translational ISF for bulk water, which is an infinite medium, and its extension to the case of confined water has been given in Ref. [18]. For a translationally invariant system, the intermediate scattering function $F_S(Q,t)$ can be derived from the van Hove self-correlation function $G_S(r,t)$ by a three-dimensional Fourier transform

$$F_S(Q,t) = \int e^{i\mathbf{Q}\cdot\mathbf{r}} G_S(r,t) d^3r. \tag{1}$$

However, imposition of a confinement breaks the translational symmetry and the van Hove self-correlation function is no longer a function of a scalar variable r. The self-correlation function $G_S(\mathbf{r},t|\mathbf{r}_0)$ now depends on both the test particle position $\mathbf{r}$ at time t and its initial position $\mathbf{r}_0$ at time zero. In this latter case the intermediate scattering function has to be calculated according to a double integral,

$$F_S(Q,t) = \int e^{i\mathbf{Q}\cdot(\mathbf{r}-\mathbf{r}_0)} G_S(\mathbf{r},t|\mathbf{r}_0) p(\mathbf{r}_0) d^3r\, d^3r_0. \tag{2}$$

The intermediate scattering function is still a function of a scalar Q due to a powder average one needs to make for an isotropic sample. In Eq. (2), $p(\mathbf{r}_0)$ is the equilibrium distribution function of the test particle under the confining potential $V(\mathbf{r})$. It is easy to see that Eq. (2) reduces to Eq. (1) in the case of an infinite medium like a bulk liquid. In this special case, $p(\mathbf{r}_0)$ is independent of the position and equals an inverse of the sample volume. $G_S(\mathbf{r},t|\mathbf{r}_0)$ is now a function of $|\mathbf{r}-\mathbf{r}_0|$ due to the translational symmetry. So the integration on the initial position can be carried out which cancels the volume factor.

Since the van Hove self-correlation function is a conditional probability of finding the test particle at $\mathbf{r}$ at time t, given that the particle was at $\mathbf{r}_0$ at time zero, there are three general properties the function has to satisfy. These in turn lead to three conditions for the ISF by its definition Eq. (2).

(i) Normalization of the probability,

$$\int G_S(\mathbf{r},t|\mathbf{r}_0)p(\mathbf{r}_0)d^3r\,d^3r_0 = 1 \qquad (3)$$

leading to $F_s(Q=0,t)=1$.

(ii) The initial condition,

$$G_S(\mathbf{r},t=0|\mathbf{r}_0)=\delta(\mathbf{r}-\mathbf{r}_0) \qquad (4)$$

leading to $F_s(Q,t=0)=1$.

(iii) Approach to a stationary distribution at sufficiently long time due to confinement,

$$G_S(\mathbf{r},t=\infty|\mathbf{r}_0)=p(\mathbf{r})=\frac{1}{Z}\exp\left[-\frac{V(\mathbf{r})}{k_BT}\right] \qquad (5)$$

leading to $F_s(Q,t=\infty)=|\int e^{i\mathbf{Q}\cdot\mathbf{r}}p(\mathbf{r})d^3r|^2$, where Z is a normalization factor defined in such a way that the volume integral of $p(\mathbf{r})$ for all space is unity. The Q-dependent factor, $A(Q)=F_s(Q,t=\infty)$, is called the elastic incoherent structure factor (EISF) and is identical to the form factor of the confining volume. We shall discuss the following two examples, which are relevant to the single-particle dynamics in supercooled water.

An analytical expression of the EISF for a test particle confined in a spherical volume of radius a can be calculated from Eq. (5) as

$$A(Q)=\left[\frac{3j_1(Qa)}{Qa}\right]^2 \approx \exp(-\tfrac{1}{3}Q^2a^2). \qquad (6)$$

If one further assumes that the test particle is diffusing inside the sphere, then the solution of the Smoluchowsky equation, which describes in general diffusion of a particle in a potential field $V(r)$, gives, to a good approximation, a translational ISF in the form [18,19]

$$F_S(Q,t)=A(Q)+[1-A(Q)]e^{-\Gamma(Q)t}. \qquad (7)$$

The corresponding self-dynamic structure factor is

$$S_S(Q,\omega)=A(Q)\delta(\omega)+[1-A(Q)]L(\omega,\Gamma), \qquad (8)$$

where $L(\omega,\Gamma)$ denotes a Lorentzian function of argument ω and half-width at half maximum (HWHM) Γ. The spectral line shape for this case is the weighted superposition of an elastic peak and a quasielastic peak which is a Lorentzian. Equation (8) was the basis for the data analysis presented in Ref. [17].

If the test particle is confined instead in a harmonic potential well, $V(r)=\tfrac{1}{2}m\omega^2r^2$, in equilibrium with a thermal bath at temperature T, the EISF in this case is usually called a Debye-Waller factor (DWF) and is given by Eq. (5) as

$$A(Q)=\exp(-\tfrac{1}{3}Q^2\langle r^2\rangle), \qquad (9)$$

where $\langle r^2\rangle=\tfrac{4}{3}(v_0^2/\omega^2)$ is the mean-square vibrational amplitude of the particle in the potential well and $v_0=\sqrt{k_BT/m}$ is the thermal speed of the particle. In a supercooled water, it is more realistic to assume that each water molecule is confined, within certain structural relaxation time, in a some-

what distorted, tetrahedrally coordinated, hydrogen-bonded cage. The configuration of the cage varies from one water molecule to another, each characterized by a different vibrational frequency ω. Thus motions of an ensemble of water molecules can be described statistically by a distribution function. This distribution function is also called the proton density of states and has been measured by a previous incoherent inelastic neutron scattering experiment of supercooled water [17]. In the relevant energy range of 0–40 meV, it shows two peaks, a prominent low-frequency peak at about 8 meV and a weak peak at about 30 meV. The frequency distribution function $Z(\omega)$ is thus simulated by an analytical function,

$$Z(\omega)=(1-C)\frac{\omega^2}{\omega_1^2\sqrt{2\pi\omega_1^2}}\exp\left(-\frac{\omega^2}{2\omega_1^2}\right)$$
$$+C\frac{\omega^2}{\omega_2^2\sqrt{2\pi\omega_2^2}}\exp\left(-\frac{\omega^2}{2\omega_2^2}\right), \qquad (10)$$

where the constant C control the relative strength of the two peaks. This function is normalized in such a way that

$$\int_0^\infty d\omega\,Z(\omega)=1. \qquad (11)$$

Under this circumstance, Chen et al. [20] has recently shown that the ISF is given by

$$F_V(Q,t)=\exp\left\{-Q^2v_0^2\left[\frac{1-C}{\omega_1^2}(1-e^{-\omega_1^2t^2/2})\right.\right.$$
$$\left.\left.+\frac{C}{\omega_2^2}(1-e^{-\omega_2^2t^2/2})\right]\right\}, \qquad (12)$$

with the corresponding DWF given by

$$A(Q)=\exp\left\{-Q^2v_0^2\left(\frac{1-C}{\omega_1^2}+\frac{C}{\omega_2^2}\right)\right\}. \qquad (13)$$

Equations (12) and (13) are both Gaussian in Q and the ISF decays to a plateau value given by $A(Q)$ within 1 ps.

Equations (7) and (12) are the ISF for a particle confined in a spherical and parabolic cage. The cage is assumed to be permanent. But in reality, in the liquid state, the cage has a finite lifetime due to the local structural relaxation. In order to take this structural relaxation into account, we shall use an idea borrowed from mode-coupling theory (MCT) of supercooled liquids. MCT is a theory that focuses its attention on the "cage effect" in the liquid state, which can be pictured as a transient trapping of molecules by their neighbors as a result of lowering of the temperature [21,22]. Microscopic test-particle density fluctuations of a disordered high-temperature liquid usually relax rapidly with a time scale of a few picoseconds. The MCT does not attempt to address the dynamics in this time regime. However, upon lowering the temperature below the freezing point, there is a rapid increase in the local order surrounding a particle, leading to a substantial increase of the local structural relaxation time. In

the supercooled liquid regime, a trapped particle in a cage can migrate only through rearrangement of a large number of particles surrounding it. There is thus a strong coupling between the test particle motion and the density fluctuations of the fluid. MCT addresses primarily physical processes in this time regime. According to MCT, the equilibrium structure factor $S(Q)$ of the liquid completely determines the long-time cage structural relaxation behavior. It predicts that on approaching a crossover temperature T_s from above, there is going to be a further separation between the time scales describing the rattling motion of a particle in the cage and the eventual structural relaxation time of the cage. At T_s the structural relaxation time becomes infinity and the supercooled liquid shows a phenomenon of structural arrest. It has been shown numerically for various model systems, such as a hard-sphere system [23] or a mixed Lennard-Jones system [24], that the time evolution of the structural relaxation (called the α relaxation) is well approximated by a stretched exponential decay.

In view of the above consideration, the realistic test-particle ISF could be constructed by multiplying the ISF's of Eq. (7) or Eq. (12) by a stretched exponential factor. From the results of the MD simulation of the SPC/E water at supercooled temperature, one found that the cage radius a in supercooled water is about 0.5 Å. Thus for a Q range between 0 and 1.0 Å^{-1}, applicable to high-resolution QENS spectra, the EISF in Eq. (6) or the DWF in Eq. (13) are very nearly unity. Thus in Eq. (7) the contribution of the second term on the right-hand side (RHS) is negligible. We can thus write with a good approximation the final ISF as

$$F_s(Q,t) = A(Q)\exp\left[-\left(\frac{t}{\tau}\right)^\beta\right]. \qquad (14)$$

This equation is appropriate also for the model of a harmonic cage. In this case the RHS of Eq. (12) reduces to Eq. (13) for the time scale of interest ($t > 1$ ps) in a high-resolution QENS experiment. Thus in this latter case we just understand the Debye-Waller factor in Eq. (14) to be that given by Eq. (13). It therefore can be concluded that Eq. (14) is a ubiquitous model for analyses of high-resolution QENS spectra. According to this relaxing cage model, there is no purely elastic line for a supercooled bulk water or an interfacial water. However, the dynamic structure factor, which is a time Fourier transform of the streched exponential function in Eq. (14), shows a sharp line near $\omega = 0$ with an extended slowly decaying side wing. This kind of line shape can also be fitted with a superposition of an elastic line and a Lorentzian quasielastic line. The way to distinguish between these two alternatives is to do absolute intensity measurements with a high spectral resolution. One then extracts the EISF or the Debye-Waller factor as a function of Q and estimates the confinement radius. This radius should have a value in the vicinity of 0.5 Å, insensitive to temperature, according to a MD simulation of SPC/E model supercooled water.

III. EXPERIMENT

A. Neutron scattering

The quasielastic neutron scattering experiments were performed at the High Flux Reactor of the Institut Laue-
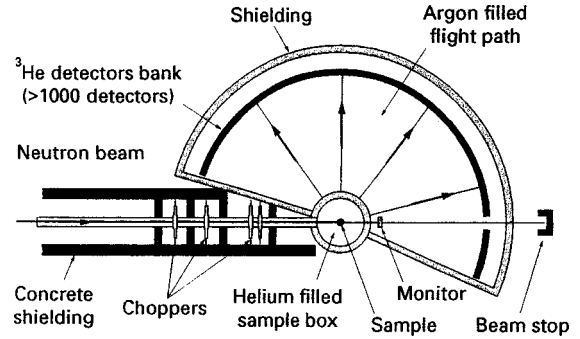

FIG. 1. Schematic diagram of IN5 multiangle chopper time-of-flight (TOF) spectrometer. It is a general purpose direct geometry TOF spectrometer which uses four synchronized disk choppers spinning at high speed to produce a pulsed monoenergetic neutron beam. Energies of the scattered neutrons are measured by their individual TOF over a fixed distance of 4 m. The sample to detector flight path is filled with argon gas to reduce losses by scattering and absorption from air. There are over 1000 He-3 detector tubes which are grouped to subtend a range of scattering angles from 11° to 130° with an angular resolution of about 20 mrad to about 70 mrad.

Langevin (ILL) in Grenoble (France) using the IN5 multidetector time-of-flight spectrometer. This is a state-of-the-art reactor based multichopper time-of-flight instrument using cold neutrons specially designed to perform quasielastic scattering measurements. The instrumental conditions were chosen in such a way as to achieve a good energy resolution at Q values less than 1 Å^{-1}. $Q = (4\pi/\lambda)\sin(\theta/2)$ is the magnitude of wave-vector transfer in the scattering where λ is the average wavelength of the incident neutrons and θ is the scattering angle. These conditions were satisfied by a choice of wavelength of the incident neutrons at 11 Å. The energy resolution (FWHM) at the elastic position was 10 μeV and the Q range covered was from 0.15 to 0.99 Å^{-1} with ten data points. A schematic spectrometer layout of the IN5 is given in Fig. 1.

In an incoherent inelastic neutron scattering experiment of a water sample containing $N/2$ molecules in the scattering volume, the measured scattered spectral intensity I_s is proportional to the incident neutron flux I_0 times a double differential scattering cross section given by

$$\frac{d^2\sigma}{d\Omega\,d\omega} = N\frac{\sigma_H}{4\pi}\frac{k}{k_0}S_s(Q,\omega);$$

$$Q = |\vec{k}_0 - \vec{k}| = \frac{4\pi}{\lambda}\sin\left(\frac{\theta}{2}\right); \quad \hbar\omega = E_0 - E, \qquad (15)$$

where $\vec{k}_0$ and E_0 are the wave vector and energy of the monochromated incident neutrons, $\vec{k}$ and E that of the scattered neutrons, Q the magnitude of the wave-vector transfer, $\hbar\omega$ the energy transfer in the scattering process, and $S_s(Q,\omega)$ the self-dynamic structure factor having a unit of seconds. The latter function has a property that its ω integral from minus infinity to infinity is unity. In practice, the scattered energy is measured by time of flight of the scattered neutron over 4 m of flight path between the sample and detectors. The time-of-flight spectra thus measured were cor-

FIG. 3. New series of high-resolution QENS data measured with 10 μeV resolution analyzed by the new model. The figure displays only the net spectral intensity of the 100% hydrated sample at $T = 278$ K. This sample, in our experience, is close to a bulk water. The empty circles are the data and the solid lines the model. Extracted parameters are listed in Table I, second column.

rected and standardized by dividing by scattering intensity from a thin vanadium plate and converted to the differential scattering cross section by using standard routines available at ILL.

B. Samples

Vycor brand porous glass no. 7930 is a product of Corning Glass Works. Vycor glass is made by heating a homogeneous mixture of boron oxide glass and silica glass above the melting point and then quenching this mixture to a temperature below the spinodal line where the mixture phase separates into two mutually interpenetrating regions. At a certain stage of preparation, the boron-rich region is leached out by acid, leaving behind a silica skeleton with a given distribution of pore sizes. The average pore size in Vycor 7930 is 50 Å, as stated by the manufacturer.

We adopted the following procedure for the preparation of the Vycor samples. The rectangular plates of Vycor were immersed in 30% hydrogen peroxide and heated to 90 °C for a few hours to remove any organic impurities absorbed by the glass. The Vycor was then washed several times in distilled water in order to remove the hydrogen peroxide and

FIG. 2. Comparison of two different methods of analyses of the same QENS data set. The spectrum was taken from a 50% hydrated sample at $Q = 1.13$ Å^{-1} and $T = 268$ K, measured with an energy resolution of 28 μeV (HWHM). (a) Analysis using the old model. The dotted-dashed line is the resolution-broadened elastic peak; the thin solid line is the resolution-broadened quasielastic peak; the dash line is the background; the solid line going through empty circles (experimental data) is a weighted sum of the elastic and quasielastic lines. (b) Analysis using the new model. The empty circles are the data; the solid line is the model. In the bottom of each figure, the difference of the measured and the theoretical spectrum is displayed. Notice the new model fits the extended wing of the spectrum slightly better.

stored in distilled water. When a hydrated Vycor sample is heated at 90 °C in vacuum until dry, it becomes translucent and clear, defining what we called a ''dry Vycor sample.'' At full hydration, a Vycor glass absorbs water up to 25% of its dry weight. A partially hydrated sample is then obtained by absorption of water in the vapor phase until the desired level of hydration is reached. The samples we used in this experiment were hydrated by H_2O to a level of 25% (i.e., 0.0625 g/g) and to 100% (i.e., 0.25 g/g). Based on the information that the dry density of Vycor is 1.45 g/ml, the porosity 28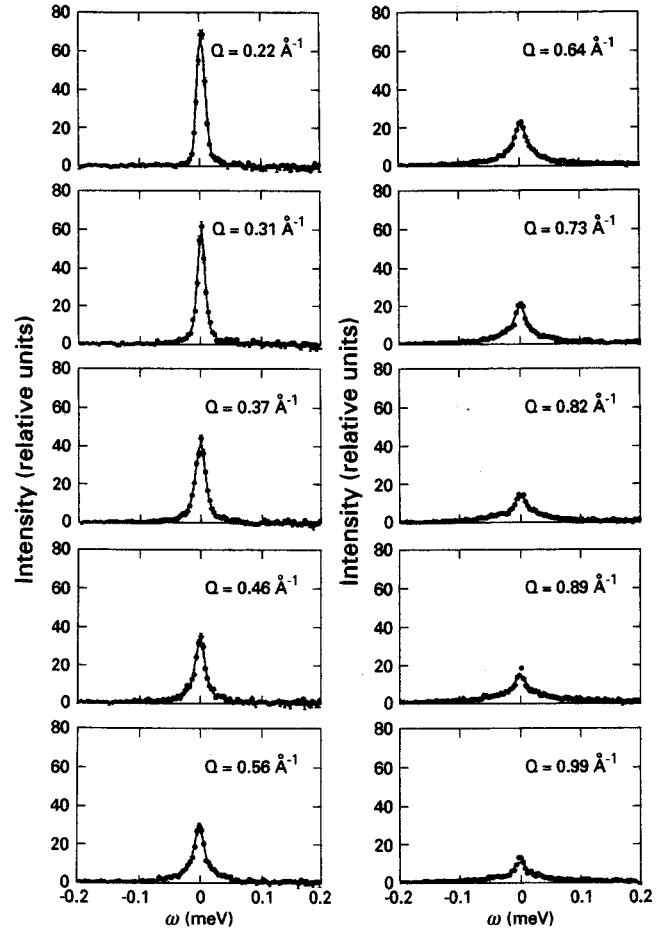%, and the internal cylindrical pores of cross-sectional diameter 50 Å, the 100% hydrated sample has three to four layers of water on its internal surface. A monolayer coverage would correspond to about 25% hydration. In order to avoid multiple scattering, the thickness of the disk-shaped Vycor plates is thinned down in such a way that neutron transmission with water inside is 90%.

The 100% hydrated sample consists of seven 0.55-mm-thick 8-mm-diam disks. These disks were folded inside an aluminum foil and placed inside an aluminum container. The dry Vycor sample was measured first at room temperature. Then the disks were unpacked and hydrated to 100% by exposure to water vapor, put back in the container, and measured at various temperatures. The 25% hydrated sample consists of rectangular plates of thickness 1.9 mm, and a surface area of 32×36 mm^2 was used.

IV. ANALYSES

Analyses were made using two models, which we called the new and the old models. A complete analysis using the old model has already been reported in Ref. [17] for a set of data taken at a medium energy resolution of 28 μeV FWHM. Part of it was reproduced here just for the sake of comparison.

The dynamic structure factor of water from the hydrated sample in the new model is written as, in accordance with Eq. (14),

$$S_{S,\text{new}}^{\text{water}}(Q,\omega) = \frac{A(Q)}{\pi} \int_0^\infty dt \cos \omega t \exp\left[-\left(\frac{t}{\tau} \right)^\beta \right]. \quad (16)$$

The Fourier transform is carried out numerically with sufficient accuracy especially around $\omega=0$. A comment should be made here about the determination of the elastic peak position, $\omega=0$. Due to slightly different orientations of the vanadium, dry Vycor, and hydrated Vycor samples with respect to the incident neutron beam, the scattered flight paths can be slightly different for each sample. This has an effect of making the time of flight of the elastic peak position of each sample slightly different. Since we shall subtract the scattering intensity of the dry Vycor from the signal of the hydrated sample, and we also shall use the normalized signal from the vanadium as the energy resolution function of the instrument, the relative positions of each elastic peak must be synchronized. We therefore take the elastic position of the hydrated sample as $\omega=0$ and adjust the elastic peak positions of the vanadium and the dry Vycor by $\omega_{\text{Res,shift}}$ and $\omega_{\text{Dry,shift}}$, respectively, so that the three peak positions all coincide at the energy transfer scale $\omega=0$. Let us denote the normalized vanadium spectral intensity $R(\omega - \omega_{\text{Res,shift}})$.
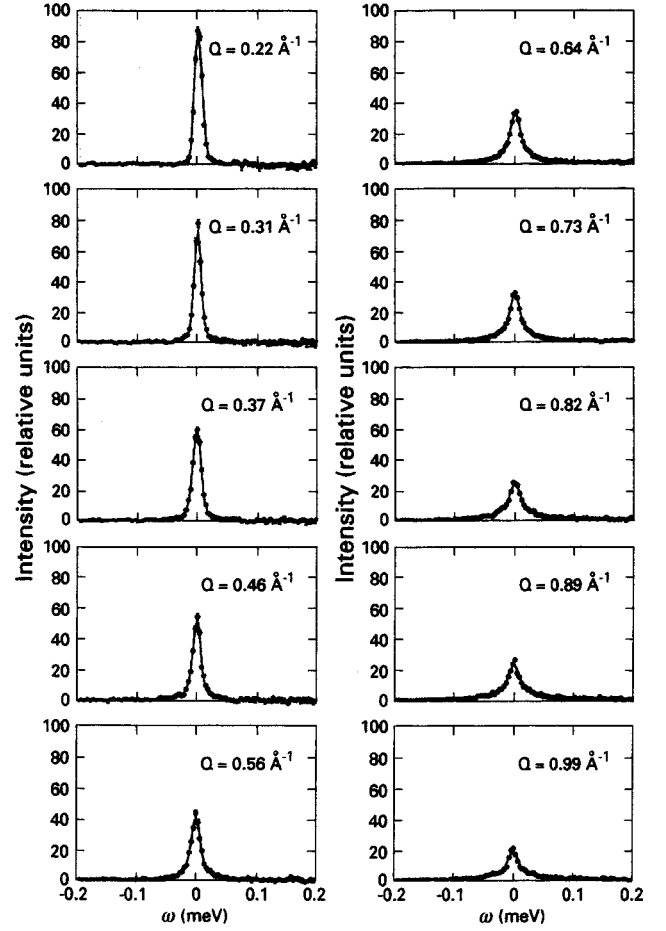
FIG. 4. New series of high-resolution QENS data measured with 10 μeV resolution analyzed by the new model. The figure displays only the net spectral intensity of the 100% hydrated sample at $T=263$ K. This sample, in our experience, is practically a bulk water. The empty circles are the data and the solid lines the model. Extracted parameters are listed in Table I, fourth column.

Then the measured, standardized (by the monitor counts) spectral intensity of the hydrated sample is fitted to an expression

$$I_{\text{Hydrated}}^M(Q,\omega) = S_{S,\text{new}}^{\text{water}}(Q,\omega) \otimes R(\omega_{\text{Van}} - \omega_{\text{Res,shift}})$$
$$+ I_{\text{Dry}}^M(Q, \omega_{\text{Dry}} - \omega_{\text{Dry,shift}}). \quad (17)$$

Thus in this model, there are five fitting parameters: $A(Q)$, τ, β, $\omega_{\text{Res,shift}}$, and $\omega_{\text{Dry,shift}}$.

The dynamic structure factor of water from the hydrated sample in the old model is, according to Eq. (8),

$$S_{S,\text{old}}^{\text{water}}(Q,\omega) = A(Q)\delta(\omega) + \frac{1-A(Q)}{\pi} \frac{\Gamma(Q)}{\omega^2 + \Gamma^2(Q)}. \quad (18)$$

The measured spectral intensity is fitted to an equation

$$I_{\text{Hydrated}}^M(Q,\omega) = S_{s,\text{old}}^{\text{water}}(Q,\omega) \otimes R(\omega_{\text{Van}} - \omega_{\text{Res,shift}})$$
$$+ I_{\text{Dry}}^M(Q, \omega_{\text{Dry}} - \omega_{\text{Dry,shift}}) + I_{\text{bgd}}, \quad (19)$$

where I_{bgd} denotes the contribution coming from ''background'' due to motions faster than 1 ps.

TABLE I. Vycor 0.25 g/g (100%) ($R = 10 \mu eV$).

Q (Å^{-1})	$T = 293$ K			$T = 278$ K			$T = 268$ K			$T = 263$ K			$T = 258$ K		
	Intensity (Rel. units)	τ (ps)	β	Intensity (Rel. units)	τ (ps)	β	Intensity (Rel. units)	τ (ps)	β	Intensity (Rel. units)	τ (ps)	β	Intensity (Rel. units)	τ (ps)	β
0.99	1.56	2.51	0.34	1.25	8.96	0.44	1.33	15.76	0.49	1.38	19.19	0.46	1.26	29.37	0.56
0.89	1.58	5.32	0.41	1.45	12.00	0.52	1.47	19.32	0.54	1.54	23.52	0.54	1.40	36.16	0.63
0.82	1.61	5.59	0.41	1.42	13.21	0.54	1.45	24.04	0.59	1.48	27.49	0.57	1.39	42.92	0.62
0.73	1.64	8.30	0.48	1.50	18.87	0.54	1.44	29.70	0.60	1.49	40.28	0.61	1.43	57.48	0.64
0.64	1.38	14.22	0.60	1.36	28.04	0.65	1.37	42.62	0.65	1.47	46.45	0.66	1.34	70.66	0.77
0.56	1.51	20.02	0.55	1.43	38.32	0.58	1.43	57.07	0.70	1.42	77.86	0.64	1.43	103.87	0.71
0.46	1.21	31.84	0.61	1.22	61.35	0.66	1.34	86.50	0.70	1.38	121.13	0.61	1.27	138.55	0.79
0.37	1.37	58.70	0.65	1.32	87.48	0.80	1.33	148.37	0.69	1.37	165.51	0.86	1.31	184.13	0.88
0.31	1.38	90.09	0.62	1.38	173.34	0.63	1.48	247.86	0.63	1.41	359.35	0.61	1.48	660.49	0.51
0.22	1.30	245.76	0.85	1.30	310.11	1.12	1.44	495.75	1.02	1.48	409.19	1.37	1.55	22 927.10	0.38

There are six fitting parameters in this model: I_{EL}, I_{QE}, $\Gamma(Q)$, $\omega_{Res,shift}$, $\omega_{Dry,shift}$, and I_{bgd}. In this new experiment, the spectrum is completely defined in the energy transfer range $-200 < \Delta E < 200 \mu eV$. The fittings procedures were applied to spectra taken at 10 scattering angles in the Q range indicated before.

In order to see the difference between the new model and the old model, we analyze an intensity spectrum, from a previous QENS experiment, at $Q = 1.13$ Å^{-1}, taken with an energy resolution of 28 μeV, covering an energy transfer range of $-200 < \Delta E < 200 \mu eV$. The results are shown in Fig. 2. The ordinate gives the spectral intensity of the net scattering from water of hydration in Vycor in a relative unit, and the coordinate is the energy transfer in units of meV. The top figure gives the result of the analysis using the old model and the bottom figure gives the result using the new model. In the bottom of each figure, we display the deviation of the measured spectrum with that of the calculated one. One sees that away from the elastic position, where the subtraction of the dry Vycor signal is not perfect, on the wing of the QENS peak, the new model fits the spectrum slightly better.

On casual inspection, the two models seem to do equally well in fitting the quasielastic peak. But a careful examination reveals a significant deviation of the old model from the data on the positive energy transfer side of the wing. Furthermore, according to the recent MD simulation of SPC/E supercooled water, the Debye-Waller factor at this Q value

should have a value close to unity. Therefore the computed quasielastic peak in the top figure ought to have a negligible area compared to that of the elastic peak. This clearly is not the case, as can be seen in the top figure. On the other hand, the bottom figure shows that the new model fits the entire line shape of the quasielastic peak very well. This point will be reinforced when we analyze the high-resolution data with the new model next.

We systematically analyze the new set of data taken with 10 μeV resolution with the new model. Figures 3 and 4 show results of the analysis for a 100% hydrated sample (0.25 g water/g Vycor) at $T = 278$ and 263 K. The ordinate is the net spectral intensity of scattering from hydration water in Vycor and the coordinate is the energy transfer in units of meV. The empty circles are the experimental data and the solid lines are the new model. One see that the agreement is very good. Table I lists all the parameters extracted from the 100% hydrated sample at four temperatures. The intensity factor is essentially the Debye-Waller factor in a relative unit. As we have noted before, the Debye-Waller factor is near unity for the indicated Q values.

We also reanalyze the 50% hydrated sample, measured with 28 μeV resolution (a previous experiment), and the 25% hydrated sample, measured with 10 μeV resolution (new series of experiments) using the new model. The extracted parameters are listed in Tables II and III. It should be commented here that, within the Q range covered by these experimental measurements and considering the error bars of

TABLE II. Vycor 0.125 g/g (50%) ($R = 28 \mu eV$).

Q (Å^{-1})	$T = 298$ K			$T = 278$ K			$T = 268$ K			$T = 258$ K			$T = 238$ K		
	Intensity (Rel. units)	τ (ps)	β	Intensity (Rel. units)	τ (ps)	β	Intensity (Rel. units)	τ (ps)	β	Intensity (Rel. units)	τ (ps)	β	Intensity (Rel. units)	τ (ps)	β
1.26	1945.60	1.17	0.34	1596.60	4.93	0.41	1503.43	9.80	0.45	1386.80	22.25	0.52	1386.80	6188.33	0.30
1.21	2031.67	1.17	0.33	1670.62	5.28	0.40	1519.31	11.46	0.46	1405.61	25.66	0.54	1405.61	4741.80	0.31
1.13	1936.56	1.67	0.35	1640.21	6.64	0.41	1487.19	14.19	0.49	1391.84	28.45	0.54	1391.84	21 268.10	0.24
0.99	1796.67	2.74	0.36	1525.99	10.21	0.44	1422.39	19.73	0.50	1343.90	38.91	0.57	1343.90	30 806.70	0.24
0.84	1567.90	5.36	0.41	1409.61	15.89	0.47	1323.46	29.29	0.54	1289.20	53.83	0.58	1289.20	178 334.0	0.19
0.74	1325.50	8.73	0.44	1221.64	22.60	0.52	1193.67	39.60	0.56	1175.05	71.32	0.59	1175.05	2 261 390.0	0.14
0.64	1192.39	12.76	0.45	1119.91	32.75	0.50	1094.43	54.55	0.54	1099.18	105.24	0.55	1099.18		
0.56	1239.89	20.66	0.46	1200.64	56.64	0.49	1198.52	95.49	0.50	1230.68	276.35	0.39	1230.68		
0.47	426.41	14.83	0.23												

TABLE III. Vycor 0.0625 g/g (25%) ($R = 10 \, \mu$eV).

Q (Å^{-1})	$T = 293$ K			$T = 278$ K			$T = 263$ K			$T = 253$ K		
	Intensity (Rel. units)	τ (ps)	β	Intensity (Rel. units)	τ (ps)	β	Intensity (Rel. units)	τ (ps)	β	Intensity (Rel. units)	τ (ps)	β
0.99	0.52	45.30	0.18	0.45	478.79	0.29	0.41	779.54	0.47	0.39	48 073.30	0.28
0.89	0.80	23.74	0.55	0.73	56.86	0.69	0.87	191.01	0.49	0.90	461.01	0.54
0.82	1.43	34.92	0.41	1.54	85.74	0.36	1.46	200.98	0.38	1.42	433.77	0.44
0.73	1.58	55.55	0.47	1.58	111.06	0.53	1.59	243.69	0.57	1.57	359.66	0.70
0.64	1.71	97.49	0.48	1.84	175.87	0.50	1.79	350.25	0.54	1.77	452.16	0.72
0.56	2.02	102.92	0.36	2.24	179.93	0.30	2.00	788.12	0.47	2.07	1427.53	0.39
0.46	1.82	141.36	0.46	1.75	293.57	0.57	1.64	521.09	0.71	1.83	643.68	0.77
0.37	2.10	382.30	0.56	2.15	460.82	0.67	2.16	560.32	1.09	2.18	789.57	0.97
0.31	2.31	3621.07	0.24	2.24	10 815.50	0.27						
0.22	3.31	6051.63	0.27	3.30	17 810.70	0.25						

various components which go into computation of the relative net spectral intensity, the Q variation of the Debye-Waller factor cannot be detected with certainty. The column in the tables denoted ''Intensity'' should be essentially constant, and any variation shown there should only reflect the level of error in the measurement of the net intensity of scattering from hydration water.

Nevertheless, experimentally significant trends of the two parameters, τ and β, as a function of Q can be extracted from this analysis. When one adopts the old model, the quasielastic peak is Lorentzian and it has been a usual practice to plot the linewidth $\Gamma(Q)$ as a function of Q^2. The reason is that it will result in a straight line with a slope D, which is the self-diffusion constant of water, in a sufficiently small Q range where the hydrodynamic limit is reached. In the new model, the quasielastic peak has a line shape which is a Fourier transform of a stretched exponential function. The spectral shape of this function near $\omega = 0$ is Gaussian with an effective width which is $1/\tau$ times some ratio of Γ functions of β. This effective width is narrower the smaller β is compared to unity. At larger ω, the shape of the spectral function

evolves into a broad wing, and the extent of it stretches as β gets smaller. Therefore, one does not have a single parameter which characterizes the linewidth. Instead one needs to discuss Q dependences of the structural relaxation rate $1/\tau$ and the stretch exponent β separately.

Figure 5 shows a plot of the structural relaxation rate as a function of Q in a linear scale for the 100% hydrated sample at five temperatures; three of the lower ones are supercooled. It is obvious that the structural relaxation rate has a power-law dependence on Q. We thus replot the same data in a log-log scale in Fig. 6. One readily sees that the data follow straight lines with positive slopes within this admittedly narrow range of Q (one decade). The values of the exponent γ are given in the inset for each temperature. One observes that the values of γ are larger than but not far from 2. The trend of the values of the exponent does not seem to agree with that of an earlier MD simulation of SPC/E water [7,8], which covered a much wider Q range. In principle, for sufficiently small values of Q, γ should reduce to 2 so that a correct hydrodynamic behavior is recovered.
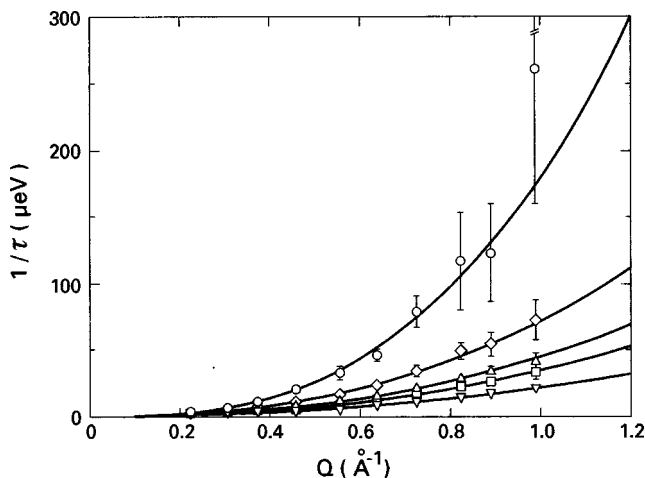

FIG. 5. Q dependence of the structural relaxation rate in units of μeV measured with 10 μeV resolution, in the 100% hydrated sample, at various temperatures. It is readily seen that the structural relaxation rate increases rapidly as Q increases. The effect is stronger at higher temperatures. $T = 293$ K ($\bigcirc$); $T = 278$ K ($\diamondsuit$); $T = 268$ K ($\triangle$); $T = 263$ K ($\square$); $T = 258$ K ($\triangledown$).
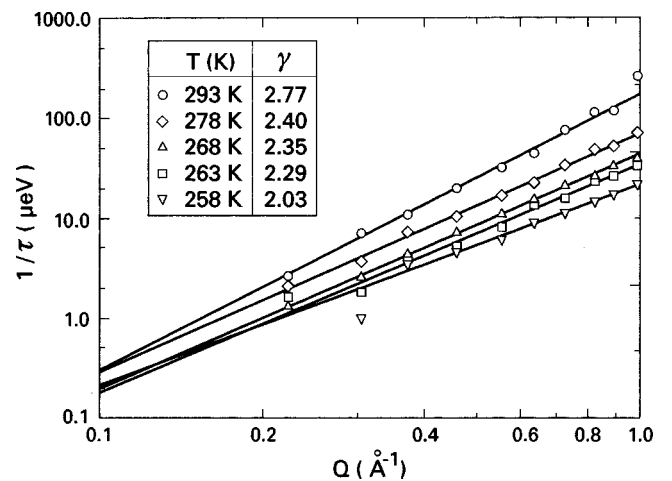

FIG. 6. Evidence of a power-law dependence of the structural relaxation rate on Q, measured with 10 μeV resolution, in the 100% hydrated sample. This graph shows a log-log plot of $1/\tau$ vs Q. Within a Q range of 0.1–1 Å^{-1}, the exponent γ, which is the slope of the solid lines joining the data points, seems to be a constant. The corresponding data from MD simulation show that the exponent γ is Q-dependent, approaching 2 as Q goes below 0.1 Å^{-1}.
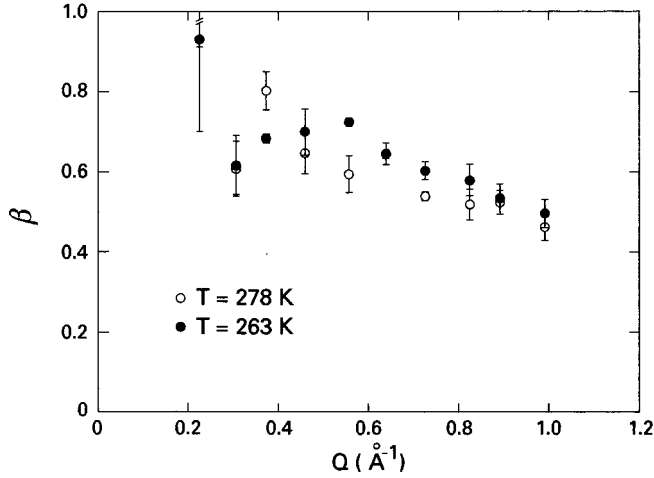
FIG. 7. Q dependence of the stretch exponent β for the 100% hydrated sample, measured with 10 μeV resolution, at two temperatures. It shows that β is lower the larger the Q values are. For $Q < 0.1$ Å^{-1}, β approaches unity, as it should be.

The Q dependence of the stretch exponent β is given in Fig. 7 for the same sample at two temperatures. It is seen that values of β are significantly below unity for large Q, but approach unity for Q less than 0.1 Å^{-1}. One can infer from these results that even at the highest temperature measured, the hydrodynamic limit is probably reached for Q only below 0.1 Å^{-1}.

Since both τ and β control the quasielastic line shape and have Q dependences, it is convenient to try to combine the two to obtain a single parameter which characterizes the structural relaxation. In the case of an exponential relaxation as a result of a continuous diffusion, one has

$$F_s(Q,t) = \exp(-DQ^2 t). \tag{20}$$
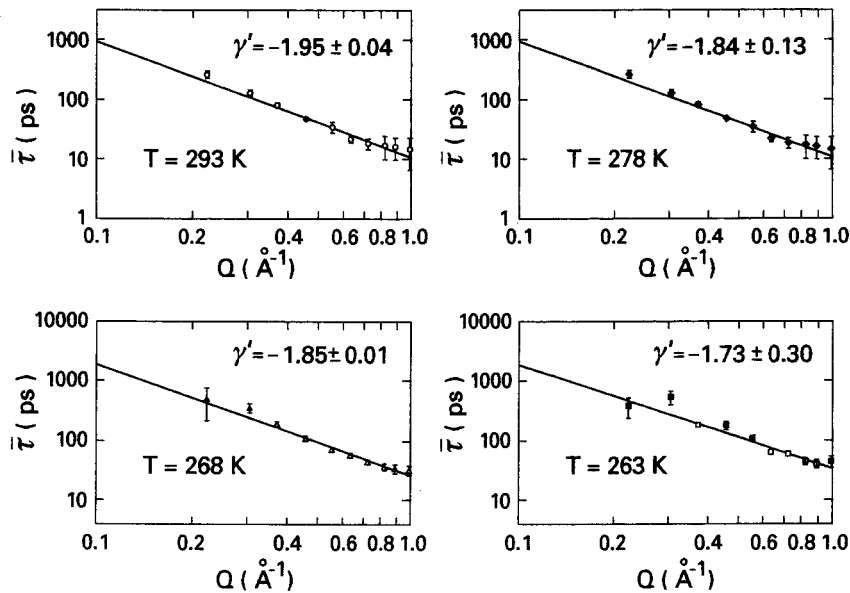
For this case, one can characterize the relaxation by its first cumulant (initial slope), which is DQ^2, or by its area, which is $1/DQ^2$. The two are equivalent. In the case of a stretched exponential relaxation, the first cumulant diverges for $\beta < 1$, but the area under the curve is [25,26]

$$\bar{\tau} = \int_0^\infty dt \exp\left[-\left(\frac{t}{\tau}\right)^\beta\right] = \frac{\tau}{\beta}\Gamma\left(\frac{1}{\beta}\right). \tag{21}$$

One may call this quantity the average relaxation time $\bar{\tau}$. It is of interest to investigate this quantity as a function of Q. Figure 8 is a log-log plot of the average relaxation time $\bar{\tau}$ as a function of Q. One sees that the average relaxation time has, within this Q range, a power-law dependence, $\bar{\tau} \approx Q^{-\gamma'}$, with an exponent γ' approximately equal to 2 at room temperature, similar to the simple diffusion case. One may then define an average diffusion constant by the relation $\bar{\tau} = 1/\bar{D}Q^2$ and use it to estimate the average diffusion coefficient $\bar{D}$. From Fig. 8, we read that for the 100% hydrated sample at 293 K, $\gamma' = -1.95$ and $\bar{\tau} = 944$ ps at $Q = 0.1$ Å^{-1}. Substituting these two numbers into the above relation, we get $\bar{D} = 1.1 \times 10^{-5}$ cm^2/sec, compared to the measured self-diffusion constant for bulk water at this temperature, which is $D = 2.0 \times 10^{-5}$ cm^2/sec. We thus arrive at a ratio $D/\bar{D} = 1.8$, agreeing with the estimate of Lee and Rossky [14] based on a MD simulation of water on a silica surface. We may also say that as far as the single-particle dynamics is concerned, water in Vycor at 293 K behaves as that in a bulk water at 273 K (20° below). As the temperature goes below the freezing point, the exponent γ' becomes less than 2, indicating a deviation from simple diffusion. A weaker Q dependence of the α-relaxation time in supercooled water was also observed in the earlier MD of SPC/E model water [7,8].

FIG. 8. Average relaxation time $\bar{\tau}$ [defined in Eq. (21)] for the 100% hydrated sample plotted against Q in log-log scales. It can be seen that the slope is approximately -2 at room temperature.

V. CONCLUSION

We have shown by analyses of an existing medium resolution QENS data and a series of new high-resolution QENS data that it is possible to treat the low-frequency spectral intensity of the incoherent neutron scattering from interfacial water as a single quasielastic peak arising from a nonexponential relaxation. It is not necessary to invoke a weighted sum of an elastic and a quasielastic peak in order to fit the complete low-frequency spectral line. With the help of results from a recent long-time MD simulation of a SPC/E bulk supercooled water, we are able to single out the translational motion of the center of mass of a water molecule as the main contributor to the incoherent quasielastic scattering peak measured with a high spectral resolution [9]. The origin of the nonexponential form of the ISF is the reflection of the diffusion process of the water molecule that is coupled strongly to and is controlled by the local structural relaxation of neighboring shells or the so-called cage effect discussed extensively in the literature dealing with mode-coupling theory of supercooled liquids. We show that a proper analysis of the QENS peak should yield three important physical parameters of interfacial water, namely the structural relaxation rate, the stretch exponent, and the Debye-Waller factor.

The main deficiency of the old model is twofold: the existence of an elastic peak is incompatible with the notion that in the liquid state water molecules must have finite mobility, and the EISF extracted from experiment is devoid of physical meaning in the sense that it gives rise to a confinement radius which is unrealistic. Due to the fact that the Q range of the measurements was restricted to below 1 Å^{-1}, a feature inherent in the kinematics of neutron scattering, in order to achieve a high spectral resolution, the Q dependence of the Debye-Waller factor could not be determined with reliability. In future experiments we hope to overcome this limitation by using different neutron spectrometers with a higher incident neutron energy so that a complete test of the new theory could be made [27].

[1] J. Teixeira, M.-C. Bellissent-Funel, S. H. Chen, and A. J. Dianoux, Phys. Rev. A **31**, 1913 (1985).

[2] S. H. Chen, in *Hydrogen-Bonded Liquids*, edited by J. C. Dore and J. Teixeira, Vol. 329 of *NATO Advanced Study Institute Series C: Mathematical and Physical Sciences* (Kluwer, Dordrecht, 1991), p. 289.

[3] S. H. Chen and J. Teixeira, Adv. Chem. Phys. **64**, 1 (1985).

[4] S.-H. Chen, K. Toukan, C. K. Loong, D. L. Price, and J. Teixeira, Phys. Rev. Lett. **53**, 1360 (1984).

[5] J. Teixeira, M. C. Bellissent-Funel, S.-H. Chen, and B. Dorner, Phys. Rev. Lett. **54**, 2681 (1985).

[6] F. Sette *et al.*, Phys. Rev. Lett. **75**, 850 (1995); **77**, 83 (1996).

[7] P. Gallo, F. Sciortino, P. Tartaglia, and S. H. Chen, Phys. Rev. Lett. **76**, 2730 (1996).

[8] F. Sciortino, P. Gallo, S. H. Chen, and P. Tartaglia, Phys. Rev. E **54**, 6331 (1996).

[9] S. H. Chen, P. Gallo, F. Sciortino, and P. Tartaglia, Phys. Rev. E **56**, 4231 (1997).

[10] F. Sciortino, L. Fabbian, S. H. Chen, and P. Tartaglia, Phys. Rev. E **56**, 5397 (1997).

[11] V. P. Denisov and B. Halle, Faraday Discuss. **103**, 227 (1996).

[12] G. Otting, E. Liepinsh, and K. Wüthrich, Science **254**, 974 (1991).

[13] C. Y. Lee, J. A. McCammon, and P. J. Rossky, J. Chem. Phys. **80**, 4448 (1984).

[14] S. H. Lee and P. J. Rossky, J. Chem. Phys. **100**, 3334 (1994).

[15] S. H. Chen, P. Gallo, and M. C. Bellissent-Funel, in *Non-Equilibrium Phenomena in Supercooled Fluids, Glasses and Amorphous Materials*, edited by M. Giordano, D. L. Leporini,

and M. P. Tosi (World Scientific, Singapore, 1996), pp. 186–194.

[16] S. H. Chen, P. Gallo, F. Sciortino, and P. Tartaglia, *Slow Dynamics in a Model and Real Supercooled Water*, in Supercooled Liquids: Advances and Novel Applications, edited by J. T. Fourkas, D. Kievelson, U. Mohanty, and K. A. Nelson, ACS Symposium Series No. 676 (ACS, Washington, DC, 1997), pp. 264–286.

[17] M. C. Bellissent-Funel, S. H. Chen, and J. M. Zanotti, Phys. Rev. E **51**, 4558 (1995).

[18] S. H. Chen and M. C. Bellissent-Funel, in *Hydrogen Bond Network*, edited by M. C. Bellissent-Funel and J. C. Dore, Vol. 435 of *NATO Advanced Study Institute Series C: Mathematical and Physical Sciences* (Kluwer, Dordrecht, 1994), p. 307.

[19] F. Volino and A. J. Dianoux, Mol. Phys. **41**, 271 (1980).

[20] S. H. Chen, C. Liao, F. Sciortino, P. Gallo, and P. Tartaglia (unpublished).

[21] E. Leutheser, Phys. Rev. A **29**, 2765 (1984); U. Bengtzelius, W. Gotze, and A. Sjolander, J. Phys. C **17**, 5915 (1984).

[22] W. Gotze and L. Sjogren, Rep. Prog. Phys. **55**, 241 (1992).

[23] M. Fuchs, I. Hofacker, and L. Latz, Phys. Rev. A **45**, 898 (1992).

[24] W. Kob and H. C. Andersen, Phys. Rev. E **51**, 4626 (1995); **52**, 4134 (1995).

[25] S. H. Chen and J. S. Huang, Phys. Rev. Lett. **55**, 1888 (1985).

[26] M. Settles and W. Doster, Faraday Discuss. **103**, 269 (1996).

[27] Very recently, S. Dellerue and M. C. Bellissent-Funel have successfully detected the presence of the DW factor which is in agreement with the value calculated by the MD [7,8]